UNIVERSITY OF BIRMINGHAM

Coherent magnetic diffraction from the uranium M4 edge in the multi-k magnet, USb

Lim, Joshua; Blackburn, Elizabeth; Beutier, Guillaume; Livet, Francis; Magnani, Nicola; Bombardi, Alessandro; Caciuffo, Roberto; Lander, G. H.

[Link to publication on Research at Birmingham portal](#)

Coherent magnetic diffraction from the uranium M_4 edge in the multi-k magnet, USb

J A Lim[1], E Blackburn[1], G Beutier[2], F Livet[2], N Magnani[3], A Bombardi[4], R Caciuffo[3] and G H Lander[3]

[1] School of Physics and Astronomy, University of Birmingham, Birmingham, B15 2TT, United Kingdom

[2] SIMaP, CNRS Grenoble-INP - UJF, Saint-Martin d'Hères, France

[3] European Commission, Joint Research Centre, Institute for Transuranium Elements, Postfach 2340, D-76125 Karlsruhe, Germany

[4] Diamond Light Source Ltd., Rutherford Appleton Laboratory, Didcot, OX11 0QX, Oxfordshire, UK

E-mail: `joshua.ajh.lim@gmail.com`

Abstract. The slow magnetic dynamics, from seconds to kiloseconds, of the canonical 3-**k** antiferromagnet USb have been probed, using X-ray photon correlation spectroscopy (XPCS). In this work, XPCS is combined with resonant X-ray diffraction to focus on scattering at an antiferromagnetic Bragg peak. High quality coherent magnetic diffraction patterns were recorded (speckle contrast of $\sim 88\%$) and magnetic domains were observed; the number of domains increases on warming to $T^* \sim 160$ K, where the spin waves soften to zero frequency, and again on warming to $T_N = 218$ K. The intensity auto-correlation, $g_2(t)$, is primarily static over 1000 s, with a small dynamical process (change of $\sim 0.4\%$) that increases in rate close to the transitions.

1. Introduction

X-ray photon correlation spectroscopy (XPCS), also known as speckle spectroscopy, uses the correlations between coherently diffracted X-rays to access dynamics on the microsecond to kilosecond timescales, with momentum resolution [1]. To date, it has primarily been used for structural studies, but close to transitions, magnetic domain wall motion should fall into the relevant time- and length-scales. However, there are only a handful of magnetic XPCS studies, concentrating primarily on antiferromagnetic domain fluctuations [2–6] in simple antiferromagnets described by a single-**k** magnetic wavevector. In these experiments, the domain structure is encoded in the time variation of a signal closely linked to the magnetic structure. For example, coherent magnetic diffraction from a purely magnetic Bragg peak will result in interference between neighbouring domains. A high resolution coherent snapshot of this Bragg peak can then be obtained - this is known as a speckle pattern. By correlating a series of these snapshots, the characteristic timescales can be extracted. Here, we present the results of an XPCS study on the actinide multi-**k** magnet, uranium antimonide.

USb is an antiferromagnet ($T_N = 218$ K) with a 3-**k** structure, meaning that three magnetic wavevectors co-exist throughout the crystal, super-imposed on a rocksalt fcc crystal structure ($a = 6.197$ Å). Indeed, USb is the canonical example of a 3-**k** magnet, after the pioneering

work of Jensen and Bak showed the spin wave spectrum could only belong to a longitudinal 3-**k** magnet [7]. The structure arises from spins pointing along local $\langle 111 \rangle$-type directions, with three equivalent wavevectors of the form [001]. This ordering acts to maintain cubic symmetry, and indeed this is confirmed by careful lattice parameter measurements [8].

The spin waves are easily observed at low temperatures, but at a temperature T^* (160 K $= T^* < T_N$) the spin wave frequency softens below the resolution limit of previous studies, and between T^* and T_N no collective excitations are observed [9, 10]. However, there is no sign of a change in the magnetic order [11, 12] and the magnetic Bragg peaks appear unaffected by this change in the dynamics [10].

Previously, it was argued [13, 14] that at T* the three independent components of the 3-**k** structure became de-phased; however, inelastic neutron scattering experiments with full polarisation analysis have shown this not to be the case [10]. In fact, the 3-**k** correlations remain even above T^* and T_N.

In a macroscopic ordered sample, it is highly likely that magnetic domains are present. Often, these arise from a need to minimise the magnetostatic energy (as is the case for ferromagnets) or due to sample topology/defects (antiferromagnets). Neighbouring domains are separated by a domain wall, which incurs some additional exchange energy cost, as well as a magnetoelastic cost due to structural differences on either side of the domain wall.

Little is known about magnetic domain dynamics in a multi-**k** system. For the case of the 3-**k** magnet, a domain wall is made of a phase slip in the magnetic propagation vector that destroys the local cubic symmetry which is necessary for, and preserved by, the 3-**k** state. For this reason, and due to exchange energy costs, the domain wall motion is expected to be relatively slow. On the other hand, in contrast to 1-**k** magnets that can couple to a lattice distortion (for example, Cr [2]), the absence of a magnetoelastic coupling in USb (i.e. pure electronic order) could result in fast domain dynamics.

The aim of this work is to use X-ray photon correlation spectroscopy to probe spatial magnetic dynamics by coherently scattering from a magnetic Bragg reflection at a resonant uranium edge from below T^* and well inside the 3-**k** state, right up to the critical regime around T_N. XPCS probes dynamics on timescales not otherwise available by other techniques, such as inelastic neutron scattering and neutron spin echo [15–17]. Previous X-ray scattering data on USb has indicated that there are multiple components to the critical scattering, with different spatial and temporal scales [18, 19].

2. Experimental Details

The key quantity obtained in an XPCS experiment is the intensity-intensity time correlation function, $g_2(\mathbf{Q}, t)$, defined as:

$$g_2(\mathbf{Q}, t) = \frac{\langle I(\mathbf{Q}, t') I(\mathbf{Q}, t' + t) \rangle}{\langle I(\mathbf{Q}, t') \rangle^2}; \ \ t \geq 0 \tag{1}$$

where $I(\mathbf{Q}, t')$ is the scattering at momentum transfer vector $\mathbf{Q}$ at a time t' and the $\langle ... \rangle$ brackets denote averages over a time t'. The time t denotes the time interval of the correlation. $g_2(\mathbf{Q}, t)$ is related to the normalised intermediate scattering function, $f(\mathbf{Q}, t)$ (which contains the sample physics) and the speckle contrast, A (a beamline dependent parameter), such that:

$$g_2(\mathbf{Q}, t) = 1 + A f(\mathbf{Q}, t)^2 \tag{2}$$

In an XPCS experiment, the speckle diffraction patterns are recorded on a CCD at time instants t' (the finite counting time of exposure is ignored here, but if treated explicitly [20] only modifies the optical contrast $A \to A'$). In this discrete limit, $g_2(\mathbf{Q}, t)$ becomes:

$$g_2(\mathbf{Q}, t) = 1 + \frac{\frac{1}{N} \sum_{t' > 0} I(\mathbf{Q}, t') I(\mathbf{Q}, t' + t)}{\langle I(\mathbf{Q}, t') \rangle^2} \tag{3}$$
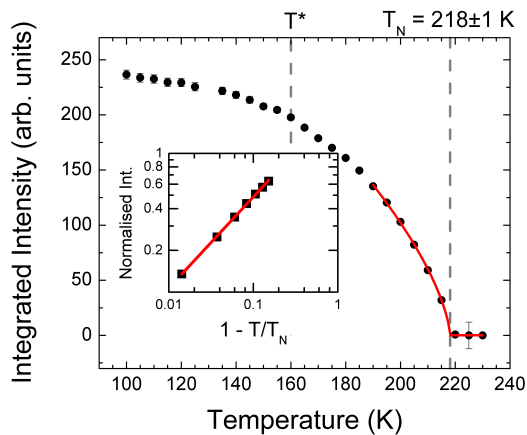
Figure 1. Integrated intensity of the **Q** = (0, 0, 3) reflection as a function of temperature, which forms a measure of the magnetic order parameter. The solid points are shown with error bars (based on the fit errors on the integrated intensity), and the solid red curve is a fit ($I = I_0 \left[1 - T/T_N \right]^{2\beta}$ with $\beta = 0.33 \pm 0.05$). Inset: log-log plot of the **Q** = (0, 0, 3) integrated intensity against reduced temperature.
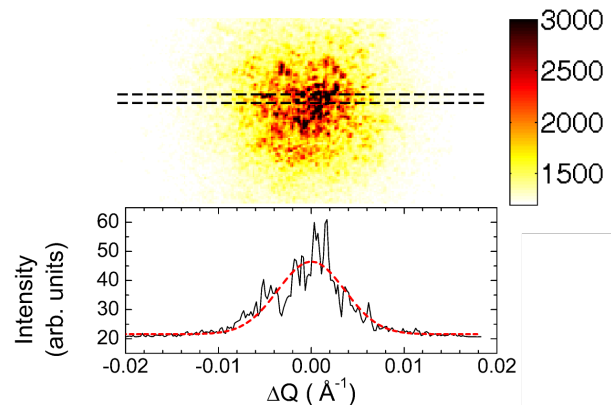
Figure 2. Upper: Typical speckle pattern obtained from the magnetic **Q** = (0, 0, 3) reflection at the M_4 resonant edge of uranium. The exposure time was 1 s and 25 x 25 μm slits were used. The black dashed lines show the region for the intensity profile in the lower panel. Lower: The intensity profile (solid line) of a slice through the speckle pattern showing intensity fluctuations that arise from the beam coherence. The red curve (Gaussian) shows the expected non-coherent intensity profile.

XPCS measurements on USb were carried out on the I16 beamline at the Diamond Light Source, UK, which was optimised for high coherence and resonant hard X-ray measurements, so is well suited for this study. The required beam coherence is generated by closing the sample slits to ~25 μm^2 (this could be optimised to maximise the number of photons whilst maintaining high coherence), 70 cm before the sample, resulting in a transverse coherence length on the order of 10μm. Excellent beam stability (no decrease in $g_2(t)$ over > 1000 s, see Fig. 4) and higher harmonic rejection was achieved with a set of slits 0.35 m upstream, acting as a secondary source, and additional mini-mirrors [21] (resulting in 0.1% of contamination from charge diffraction from higher harmonics at the **Q** = (0, 0, 3) position).

The key feature of the setup was an extension of the detector arm, by including a section of evacuated PVC pipe capped with Kapton® windows (detector-sample distance was 1.26 m). This was necessary to obtain high enough resolution on the detector to resolve the speckles over multiple pixels on the camera. The extension was evacuated to reduce losses and noise from air scattering. The detector used to capture snapshots of the speckle pattern was an ANDOR® iKon-M 934 (1024 x 1024 13 μm pixels), continuously cooled at -65°C.

The sample was a high quality single crystal of dimensions $2 \times 2 \times 2$ mm, with polished faces. The average mosaic width was 0.08° at full width half maximum and the sample was mounted on a copper puck using silver paint to ensure good thermal contact and stability. Pure magnetic reflections from the uranium M_4 edge (3.728 keV) provide a large enhancement of the magnetic scattering [22], enough to mitigate against the loss of intensity from a pinhole aperture. The feasibility of this approach had been demonstrated by preliminary studies on the isostructural compound UAs at the ESRF where, in similar conditions, up to 2000 cts/s from
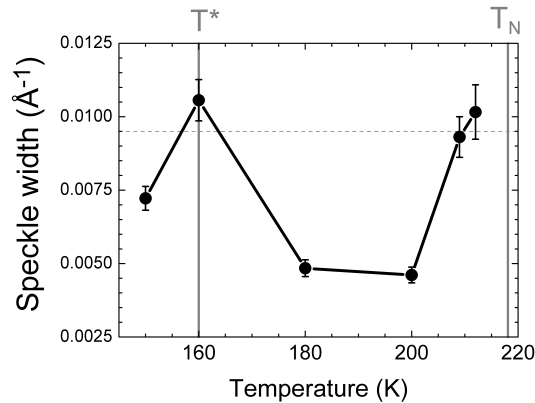
Figure 3. The extracted FWHM of the magnetic speckle pattern as a function of temperature. This is related to the average domain size and implies a decrease in the real space domain size around T^* and T_N (marked by vertical lines). The dashed horizontal line denotes the FWHM from the $\mathbf{Q} = (0, 0, 2)$ reflection, as measured at 100 K.

the $\mathbf{Q} = (0, 0, 1)$ reflection and static speckles were observable [6]. The scattering can be further enhanced by measuring at $\mathbf{Q} = (0, 0, 3)$ ($2\theta = 107.6°$), where there is a nine times intensity gain over the $\mathbf{Q} = (0, 0, 1)$ [23]. It can be seen from Eq. (15) in reference [23] that if the structure is longitudinal, as in USb, the scattering cross section is proportional to $\sin^2(\theta)$, where θ is the Bragg angle. Hence the large increase in the magnetic scattering at high Bragg angle.

The energy resolution of the setup at the M_4 edge was 4.0 ± 0.2 eV at full width at half maximum [24], corresponding to a longitudinal coherence length of $\sim 4\mu m$ that is comparable to the maximum optical path difference (governed by the X-ray attenuation length and scattering geometry).

Snapshots of the speckle pattern were recorded at six different temperatures from 150 K (where we expected slow dynamics and few domains) to above both T^* and T_N (where there are expected to be many domains). Close to the transitions and in the critical regime, we expected the dynamics to slow dramatically [2–5]. Exposure times of 1, 3 and 10 seconds were used. By correlating series of images at fixed temperature, it was possible to calculate the intensity autocorrelation function to look for the characteristic timescale of the magnetic fluctuations. Speckle images were recorded 10 minutes after changing temperature; however at least 1 hour was left for the setup to stabilise, which was justified by checking that the individual values of $g_2(t)$ against acquisition time showed a random, and not a transient, response.

The calculation of $g_2(t)$ for each temperature typically used 1000 frames (where available), which corresponds to a dynamic range from ~ 1 second to 1 hour, although dynamics could only be reliably extracted to ~ 1000 s. No evidence for any ΔQ dependence to $g_2(t)$ was found, similar to other reported magnetic XPCS studies [2–5] and the whole speckle pattern was used for correlation to improve statistics. The results were independent of choosing overly large regions for analysis, due to a thresholding procedure that meant pixels with low counts did not increase the noise background [25]. A scheme using the droplet algorithm [26, 27] to count photons gave supporting results, although is not presented in this analysis.

3. Results and Discussion
The 3-**k** order parameter was measured by rocking the sample through the Bragg condition at $\mathbf{Q} = (0, 0, 3)$ position and integrating the intensity using a Voigt function (see Fig. 1). The integrated intensity near the transition was fitted with a general order parameter function
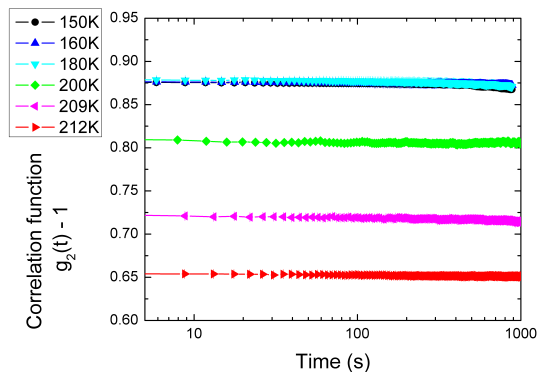
Figure 4. The calculated correlation function, $g_2(t)$, for different temperatures (error bars displayed) showing largely a static response.
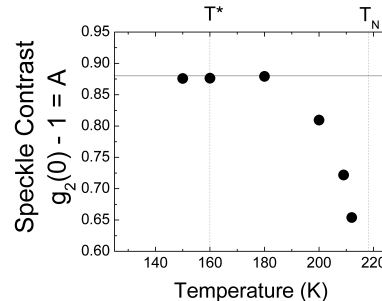
Figure 5. Magnetic speckle contrast as a function of temperature, which shows a maximum (the solid line) at $A = 0.88$.

$[I = I_0(1 - T/T_N)^{2\beta}]$ and the critical exponent, $\beta = 0.33 \pm 0.05$ and Néel temperature, $T_N = 218 \pm 1$ K were extracted, showing close agreement with published values [10, 19, 28, 29]. At the $\mathbf{Q} = (0, 0, 3)$ position for 150 K, an average of 8800 photons per second were measured.

The upper panel of figure 2 shows a typical speckle pattern, in this case measured at 150 K, that has clear and well-defined speckles. The lower panel of figure 2 shows an intensity slice through the centre of this pattern. The solid red curve (Gaussian) shows the expected diffracted intensity profile for non-coherent scattering. The large intensity fluctuations and fine structure relative to this curve indicate the high coherence and speckle contrast of the setup.

The spread of the speckle pattern on the CCD also gives information about the characteristic length scales of the magnetic domains. The central intensity profiles of the speckle patterns fit well to a Lorentzian lineshape, and the half width at half maximum, ΔQ, is partly related to the average domain size. This quantity ΔQ is a convolution of the mosaic width and the domain size. These quantities have a different Q-dependence, but with long wave-length X-rays the observations in the present experiment are too restricted to be able to separate them. The mosaic width is not expected to change with temperature, so variations in ΔQ can be interpreted as changes in the domain size.

The temperature dependence of the FWHM of the magnetic speckle pattern is shown in Figure 3. For comparison, the ΔQ spread of the structural reflections [as measured from the $\mathbf{Q} = (0, 0, 2)$ peak] is always larger than the magnetic reflections, suggesting the magnetic domain size is not limited by the structure: a feature also observed in UAs [6]. The temperature dependence shows an increase in the FWHM of the magnetic reflections close to T_N and T^* corresponding to a decrease in the magnetic domain size. Near T_N this behaviour is expected as the sample fragments into many smaller 3-$\mathbf{k}$ domains. Interestingly, this behaviour is also seen near T^* which indicates there are also changes to the domain configurations around this temperature.

From auto-correlation of the speckle patterns, $g_2(t)$ was calculated and the results (see Fig. 4) show that the correlations do not change significantly with time.

The coherence contrast can be estimated to be equal to A [recall $g_2(t) = 1 + Af(\mathbf{Q}, t)^2$ (Eqn. 2)] and at low temperatures (< 180 K) this saturates at a maximum, $A = 0.88$. The contrast was found to decrease with the scattered flux [6], but does not follow the same scaling relationship as the order parameter, indicating that other factors are also at play (see Fig. 5). High contrast for the $\mathbf{Q} = (0, 0, 2)$ charge peak was measured ($A = 0.93$) due to the increased flux and reduced 10 x 10μm slits. Nonetheless, the constant response of $g_2(t)$ reflects the excellent stability of the
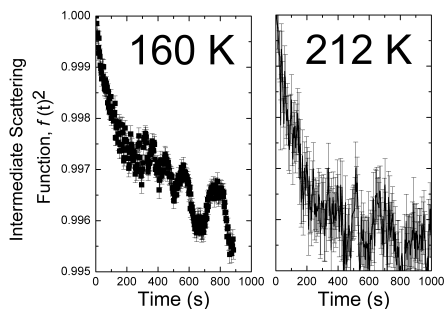
Figure 6. The normalised correlation response (the intermediate scattering function, $f(t)^2$), at temperatures near T^* and T_N zoomed in and showing the small decrease in correlation with increasing time.
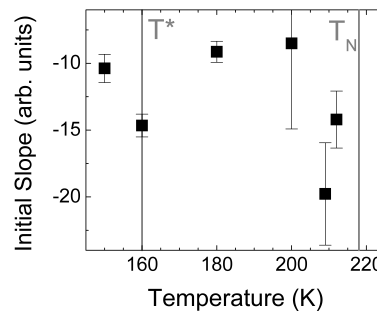
Figure 7. The initial linear gradient of the intermediate scattering function against temperature (greater negative gradient corresponds to faster dynamics) showing faster dynamics near T^* and T_N (denoted by vertical lines).

setup on I16 and the high speckle contrast shows the suitability of this beamline for correlation spectroscopy over hundreds of seconds.

This apparent time independent result corresponds with visual inspection of the speckles that appear to be static, reflecting the large static magnetisation of the 3-**k** state. As discussed earlier, the reason for the slow and quasi-static response in comparison with other 1-**k** magnetic studies may be due to the additional cubic symmetry breaking constraint of the domain wall in the 3-**k** state. Zooming in on $g_2(t)$ we see more detail and evidence for a small relaxation (see Fig. 6). At longer times, the oscillatory signal visible at 160 K is unlikely to be linked to the sample physics, but is possibly due to a property of the beamline setup.

We note that in contrast to other magnetic XPCS studies where the correlation function drops towards zero for long times [2, 5]), this is not observed in USb. We argue that this is due to static magnetic domains; however we cannot rule out small and fast fluctuations, which do not appreciably change the recorded speckle pattern or are outside of the time interval probed by this technique.

It was not possible to fit the response for all the obtained curves (nor was it always possible to clearly resolve the functional form [2, 3, 5]). A proxy for the relaxation dynamics was estimated by looking at the initial linear slope from the first 100 s (Fig. 7). This shows evidence for a faster dynamical response around T_N as expected, and also a small increase in the rate of relaxation around T^*. This dynamical picture supports the static speckle information which gives evidence for a change in the domain configuration around T_N and also T^* (see Fig. 3).

Using XPCS, we have observed a very slow response to domain motion, whilst the characteristic energies of the spin waves place the associated times in the giga-hertz regime. For this reason, it is unlikely that the changes to the magnetic domains are driving the physics at T^*, rather it appears the decrease in magnetic domain size and increase in fluctuations reflects the spin wave mode softening. It is interesting to note that this behaviour at T^*, which has been attributed to a change in itinerancy [10], can also result in changes to the magnetic domains.

4. Summary and conclusions

High quality speckle patterns were measured at the uranium M_4 resonant edge in bulk USb samples from the purely magnetic $\mathbf{Q} = (0, 0, 3)$ reflection, that showed high stability and an almost static response. The speckle contrast was found to be $\sim 88\%$ in the setup using a pinhole aperture of 25 x 25 μm and demonstrates the suitability of I16 in this setup for studying

magnetic domain dynamics.

There are clear change in the static and dynamical speckle patterns that show an increase in fluctuations and decrease in domain size around T_N and T^*. The cause behind the change of behaviour around T^* remains unclear, although this work shows that physics at T^* cannot only be understood by changes in itinerancy [10].

In contrast to 1-**k** magnets that show a large change in correlations and dynamics readily accessible in the sub-1000 seconds time window [2–5], in USb the magnetic domains appear static and the fluctuations slow.

These results are among the first XPCS measurements on a $5f$ electron system and this is one of the few studies to look at domains in a multi-**k** magnet. This work shows the potential of the XPCS technique which combines coherent X-rays and resonant diffraction, for study of domain dynamics that is not otherwise accessible by other means.

Acknowledgments

References
[1] Grübel G and Zontone F 2004 *Journal of Alloys and Compounds* **362** 3 – 11 ISSN 0925-8388 proceedings of the Sixth International School and Symposium on Synchrotron Radiation in Natural Science (ISSRNS)
[2] Shpyrko O, Isaacs E, Logan J, Feng Y, Aeppli G, Jaramillo R, Kim H, Rosenbaum T, Zschack P, Sprung M et al. 2007 *Nature* **447** 68–71
[3] Seu K A, Roy S, Turner J J, Park S, Falco C M and Kevan S D 2010 *Phys. Rev. B* **82**(1) 012404
[4] Konings S, Schüßler-Langeheine C, Ott H, Weschke E, Schierle E, Zabel H and Goedkoop J B 2011 *Phys. Rev. Lett.* **106**(7) 077402
[5] Chen S W, Guo H, Seu K A, Dumesnil K, Roy S and Sinha S K 2013 *Phys. Rev. Lett.* **110**(21) 217201
[6] Yakhou F, Létoublon A, Livet F, De Boissieu M and Bley F 2001 *Journal of magnetism and magnetic materials* **233** 119–122
[7] Jensen J and Bak P 1981 *Phys. Rev. B* **23**(11) 6180–6183
[8] Knott H W, Lander G H, Mueller M H and Vogt O 1980 *Phys. Rev. B* **21**(9) 4159–4165
[9] Hagen M, Stirling W G and Lander G H 1988 *Phys. Rev. B* **37**(4) 1846–1859
[10] Lim J A, Blackburn E, Magnani N, Hiess A, Regnault L P, Caciuffo R and Lander G H 2013 *Phys. Rev. B* **87**(6) 064421
[11] Schoenes J, Frick B and Vogt O 1984 *Phys. Rev. B* **30**(11) 6578–6585
[12] Ochiai A, Suzuki Y, Shikama T, Suzuki K, Hotta E, Haga Y and Suzuki T 1994 *Physica B: Condensed Matter* **199** 616 – 618 ISSN 0921-4526
[13] Asch L, Kalvius G M, Kratzer A and Litterst F J 1994 *Hyperfine Interactions* **85**(1) 193–196 ISSN 0304-3843
[14] Lander G H and Burlet P 1995 *Physica B: Condensed Matter* **215** 7 – 21 ISSN 0921-4526
[15] Mezei F 2003 *Neutron spin echo spectroscopy* (Springer)
[16] Pappas C, Mezei F, Triolo A and Zorn R 2005 *Physica B: Condensed Matter* **356** 206 – 212 ISSN 0921-4526
[17] Squires G L 1978 *Introduction to the theory of thermal neutron scattering* (Cambridge University Press)
[18] Perry S C, Nuttall W J, Stirling W G, Lander G H and Vogt O 1996 *Phys. Rev. B* **54**(21) 15234–15237
[19] Nuttall W, Perry S, Stirling W, Mitchell P, Kilcoyne S and Cywinski R 2002 *Physica B: Condensed Matter* **315** 179 – 186 ISSN 0921-4526
[20] Jakeman E 1973 *Photon Correlation and Light Beating Spectroscopy* (Plenum, New York)
[21] Aranda M A G, Berenguer F, Bean R J, Shi X, Xiong G, Collins S P, Nave C and Robinson I K 2010 *Journal of Synchrotron Radiation* **17** 751–760
[22] Tang C C, Stirling W G, Lander G H, Gibbs D, Herzog W, Carra P, Thole B T, Mattenberger K and Vogt O 1992 *Phys. Rev. B* **46**(9) 5287–5297
[23] Hill J P and McMorrow D F 1996 *Acta Crystallographica Section A: Foundations of Crystallography* **52** 236–244
[24] Bao Z, Springell R, Walker H, Leiste H, Kuebel K, Prang R, Nisbet G, Langridge S, Ward R, Gouder T, Caciuffo R and Lander G 2013 *Physical Review B* **88** 134426
[25] Lumma D, Lurio L B, Mochrie S G J and Sutton M 2000 *Review of Scientific Instruments* **71** 3274–3289
[26] Beutier G, van der Laan G, Marty A and Livet F 2008 *The European Physical Journal Applied Physics* **42**(02) 161–167 ISSN 1286-0050

[27] Livet F, Bley F, Mainville J, Caudron R, Mochrie S, Geissler E, Dolino G, Abernathy D, Grübel G and Sutton M 2000 *Nuclear Instruments and Methods in Physics Research Section A: Accelerators, Spectrometers, Detectors and Associated Equipment* **451** 596 – 609 ISSN 0168-9002

[28] Knott H W, Lander G H, Mueller M H and Vogt O 1980 *Phys. Rev. B* **21**(9) 4159–4165

[29] Lander G H, Sinha S K, Sparlin D M and Vogt O 1978 *Phys. Rev. Lett.* **40**(8) 523–526